THE ASTRONOMICAL JOURNAL VOLUME 93, NUMBER 6 JUNE 1987

THE CENTAURUS-HYDRA SUPERCLUSTER REGION. II

L. N. DA COSTA, C. WILLMER, AND P. S. PELLEGRINI
Department of Astronomy, CNPq/Observatório Nacional, Rua General Bruce, 586, Sao Cristovao 20921, Rio de Janeiro, Brazil

G. CHINCARINI[a]
Universitá di Milano e Osservatorio Astronomico di Brera, Milan, Italy
Received 23 December 1986

ABSTRACT

In this paper, we present 139 redshifts obtained in the region of the Centaurus-Hydra supercluster. These data, combined with the radial velocities reported in an earlier paper, are used in a preliminary investigation of the spatial distribution of galaxies in the surroundings of the Centaurus cluster. We focus our attention on two particular regions of the sky for which we have nearly complete redshift samples of galaxies brighter than blue magnitude 15.0. From the analysis of the spatial distribution of galaxies in these two regions, we find that the system of galaxies associated with the Centaurus cluster extends northeastward, and that the complexes of Centaurus and Hydra may well be considered as separate superclusters.

I. INTRODUCTION

In recent years, an increasing number of investigators have become interested in the study of the Centaurus-Hydra supercluster (CH). This interest has been motivated primarily because it is, apart from Virgo, the closest large-scale structure in the nearby volume of space, making it ideal for detailed structural and morphological studies. Furthermore, its proximity may have a bearing on the kinematics of the Local Group. In particular, in order to reconcile the motion of the Local Group, as derived from the measurements of the microwave-background dipole anisotropy, with a low infall velocity towards Virgo one must require the existence of a density perturbation in the direction $l = 274°$, $b = 12°$, close to the nominal center of the CH complex (Tammann and Sandage 1985).

Although the existence of the Centaurus-Hydra supercluster has been recognized for some time (Chincarini and Rood 1979), until recently the available radial-velocity data in its general direction were rather sparse. The limited amount of data has thus prevented attempts to investigate in greater detail the geometry, extension, and relative importance of the density perturbation associated with the CH complex. In the last few years, the situation has begun to change with the new data that have become available from the several ongoing survey efforts in this region. These surveys still have a limited sky coverage, with most of the data being primarily collected in the neighborhood of the richest groups and clusters such as Hydra (Richter *et al.* 1982; Richter and Huchtmeier 1983), Centaurus (Dickens *et al.* 1986), Klemola 27 (Richter 1984), and Antlia (Hopp and Materne 1985). Despite these important contributions, a more complete survey of CH is still necessary and must be pursued. It was for this reason that we initiated a few years ago a redshift survey of the CH region (da Costa *et al.* 1986, Paper I), which complements the ongoing redshift survey of the southern galactic cap (da Costa *et al.* 1984). However, due to the slow progress of the observations, our strategy has been, so far, to complete magnitude-limited samples in two selected regions. These regions were chosen with the purpose of further investigating the impression obtained from the analysis of the projected galaxy distribution, that the Centaurus system may extend towards the northeast, and that it may not be connected to the Hydra complex (Paper I). In order to confirm these results, in this paper we investigate the three-dimensional distribution of galaxies in these selected regions, using the new redshifts reported here and in Paper I, which combined provide a database of 250 redshifts in the direction of the CH complex.

In Sec. II, we describe the procedure adopted to assign provisional magnitudes to the galaxies drawn from the ESO/Uppsala catalog (Lauberts 1982), in an attempt to define magnitude-limited samples suitable for analysis. In this section we also list 139 new redshifts obtained in the CH direction. In Sec. III, we discuss the main features of the spatial distribution of galaxies in the selected regions and in the vicinity of the Centaurus cluster. Finally, in Sec. IV we give a brief description of the overall structure of the CH supercluster based on all the presently available data.

II. THE DATA

We concentrated our observations in the following regions:

$$\text{Region I} \quad \begin{array}{c} 13^{h} \leqslant \alpha \leqslant 14^{h} \\ -33° \leqslant \delta \leqslant -25°, \end{array}$$

$$\text{Region II} \quad \begin{array}{c} 11^{h} \leqslant \alpha \leqslant 12^{h} \\ -33° \leqslant \delta \leqslant -27°. \end{array}$$

These regions were selected in order to investigate whether the apparent concentration of galaxies to the northeast of the Centaurus cluster is indeed associated with it, as suggested by the distribution plotted in Fig. 1 of Paper I, and to search for a low-density component connecting the Centaurus and Hydra complexes.

Galaxies in the regions of interest were drawn from the diameter-limited ESO/Uppsala catalog, which provides information for galaxies with major diameters $\geqslant 1'$. In order to use a magnitude-limited sample, we have assigned to each galaxy tentative blue magnitudes m_b based on mean relations between magnitudes and diameters. These relations were derived by linear least-square fits to the data points available from all galaxies in the catalog with listed B_T magnitudes and $b \leqslant -30°$. These magnitudes were converted to

[a] On leave of absence from the University of Oklahoma.

 0004-6256/87/061338-12$00.90

the $B(0)$ system (de Vaucouleurs and de Vaucouleurs 1964) and correlated with the face-on major diameters $D_{25}(0)$ (de Vaucouleurs *et al.* 1976) obtained from the major and minor diameters listed in the ESO/Uppsala catalog using the conversion proposed by Fouqué and Paturel (1985). We chose to use the $B(0)$ system in order to be as close as possible to the $B(0) - \mathrm{ZGC}$ system (Huchra 1976) adopted in the CfA Redshift Survey (Huchra *et al.* 1983), one of the largest existing surveys of the northern hemisphere.

The procedure used here for estimating magnitudes is similar to that used by Hopp and Materne (1985) but, unlike these authors, we divided the sample of galaxies with photometric information into different morphological type groups and derived separate magnitude-diameter relations. While this was done in an attempt to minimize the scatter, we find that the estimated errors in magnitudes are still large, ranging from 0.5 to 0.7 mag for the different morphological type groups utilized. However, we believe that our procedure has the advantage of minimizing the morphology-dependent effects that would be introduced if a magnitude-limited sample were drawn from a diameter-limited catalog based on a single relation between these quantities. This is because, for a given diameter, the corresponding magnitude should depend on the morphological type (mean surface brightness) of the galaxy considered. An example of this effect has been discussed by Sadler (1984), who concluded that the sample of E and S0 galaxies may become incomplete near $B_{\mathrm{T}} = 14.0$ ($m_B \sim 14.5$) because early-type galaxies fainter than this magnitude have in general diameters that fall below the cutoff diameter of the ESO/Uppsala Catalog.

Using the magnitude system described here, the samples considered for analysis consisted of all galaxies brighter than $m_B = 15.0$, although we also present redshifts for galaxies fainter than this limit in both papers. The total number of galaxies brighter than 15.0 is 149 in region I and 36 in region II. We note that since the number of early-type galaxies is underestimated for magnitudes fainter than $m_b = 14.5$, the values for the completeness of the galaxy samples mentioned below refer only to that of the magnitude-limited samples as defined above. However, the incompleteness of early-type galaxies in the sample, which can only be overcome once a deep photometric survey becomes available, is not expected to affect in a significant way the conclusions reached in the present paper about the general characteristics of the galaxy distribution.

In Table I we list a total of 139 new heliocentric velocities in the general direction of the Centaurus complex. In this table we list radial velocities for 79 galaxies in region I, 27 in region II, and 33 in the general vicinity of the Centaurus cluster. Combining these measurements with those available in Paper I and in the literature, we find that the sample of region I, where we have measured redshifts for 118 galaxies with $m_B \leqslant 15.0$, is complete to that limit. In region II there are redshifts for 33 of the 36 galaxies with $m_B \leqslant 15.0$, of which 23 are new measurements listed in Table I. We also obtained long-exposure spectra for the three remaining low-surface-brightness galaxies (ESO 438 G10, ESO 439 G11, and ESO 504 G25), but the measured velocities are rather uncertain and were not included in Table I.

The new radial velocities reported in the present work were obtained and reduced using the same equipment and data-reduction techniques as described in Paper I, and have a typical error of less than 40 km s^{-1}. In the subsequent sections, all velocities have been corrected for 300 km s^{-1} galactic rotation and for a dipole Virgocentric flow, with an assumed infall velocity of 300 km s^{-1} (Geller and Huchra 1983).

III. THREE-DIMENSIONAL GALAXY DISTRIBUTION

a) Distribution of Galaxies in the Selected Regions

The distribution in radial velocity for the galaxies in region I brighter than $m_B = 15.0$ is shown in Fig. 1. The superimposed solid curve is the expected velocity distribution for a uniform sample described by the Schechter (1976) form of the luminosity function, using the parameters $M_* = -19.4$ and $\alpha = -1.3$ (Davis and Huchra 1982, DH) and normalized to the total number of observed galaxies. The distribution of observed redshifts shows the presence of features indicative of clustering at different radial velocities. This figure is similar to that shown in Paper I, except that the sample considered here is magnitude limited and only includes galaxies strictly within region I. The main features of the histogram are: a foreground group at about 500 km s^{-1}; a clustering at about 2000 km s^{-1}; a significant excess of galaxies at about 4000 km s^{-1}, close to the mean radial velocity of the Centaurus cluster; the suggestion of an underdense region beyond 6000 km s^{-1}; the presence of possibly two background structures at about 10 000 km s^{-1} and 14 000 km s^{-1}.

The nature of the large-scale clustering in region I can be examined in more detail in the cone diagrams shown in Fig. 2. The largest system in the region is Klemola 27 (13.7^{h}, $-30°$) at about 4600 km s^{-1}. Other smaller systems can also be recognized such as the foreground NGC 5128 group (13.5^{h}, $-37°$, 500 km s^{-1}), the NGC 4936 group (13.0^{h}, $-30°$, 3200 km s^{-1}), and the IC 4296 group (13.5^{h}, $-33°$, 3900 km s^{-1}) near the southern border of the surveyed region. The distribution in redshift space clearly shows a concentration of galaxies in the velocity interval between 3500 km s^{-1} and 6000 km s^{-1}, already suggested in Fig. 1. In fact, when all the available data are examined, one finds that this concentration stretches across the sky beyond the surveyed solid angle, at least to the position of the cluster located at 14^{h} and $-33°$, identified as the NGC 5419 group at about 4300 km s^{-1}. At the mean distance of this structure, the observed angular size corresponds to a linear scale of at least $10h^{-1}$ Mpc ($H_0 = 100h^{-1}$ km s^{-1}/Mpc). Other interesting features of Fig. 2(a) are the existence of two apparently empty regions in the surveyed region, one spanning 1000 km s^{-1} separating the clustering at about 2000 km s^{-1} from that at 4000 km s^{-1}, and another stretching for at least 3000 km s^{-1} beyond about 5500 km s^{-1}. From Fig. 2(b) we also see that the observed complex of galaxies seems to lie preferentially on a sheet with an apparent width of about $2h^{-1}$ Mpc.

In order to confirm this qualitative description, we have calculated the radial variation of the spatial density of bright galaxies ($M_B \leqslant -18.5$), following the procedure outlined by DH, which takes into account the observational bias of a magnitude-limited sample. The density function averaged over the solid angle was calculated from the expression

$$n(r) = N(r)/(\omega r^2 \phi(r) \Delta r), \qquad (1)$$

where $N(r)$ is the number of galaxies in a shell of thickness Δr (2 Mpc) at radius r, ω the solid angle of the surveyed region, and $\phi(r)$ the selection function which has been cal-

TABLE I. Redshift data.

ESO NO.		OTHER ID.	R.A. H	M	S	DEC. O	'	V (KM/S)	±
438	G 11		11	9	3	-30	50.0	9983	42
438	G 12	MCG-5-27-1	11	9	51	-27	43.7	1322	29
438	G 15	MCG-5-27-3	11	12	37	-28	7.1	3385	30
503	G 5		11	12	49	-27	23.3	3961	26
503	G 7	MCG-4-27-6	11	13	22	-26	50.3	1517	23
438	G 19	MCG-5-27-6	11	15	7	-30	14.9	9839	33
438	G 20	MCG-5-27-9	11	16	27	-29	9.1	9081	29
438	G 23	MCG-5-27-10	11	18	26	-29	7.7	8917	28
439	G 1		11	19	3	-32	29.6	17155	33
439	G 5		11	21	57	-29	41.0	9013	26
439	G 8	I 2764	11	24	37	-28	42.2	1627	28
439	G 10		11	25	4	-28	54.1	7164	43
439	G 12		11	26	39	-29	18.4	749	49
439	G 13	MCG-5-27-14	11	27	15	-31	34.5	8977	35
439	G 14		11	27	29	-31	29.5	9208	31
439	G 17		11	29	34	-31	48.1	3849	37
503	G 22	MCG-4-27-12	11	31	0	-26	40.3	1911	30
439	G 18	MCG-5-28-1	11	35	31	-32	2.9	8887	28
439	G 20	MCG-5-28-3	11	35	46	-29	27.1	4185	29
440	G 1		11	41	55	-28	11.2	8571	32
440	G 4		11	43	11	-28	5.4	1836	38
440	G 6	MCG-5-28-5	11	44	1	-29	49.3	1754	33
504	G 16		11	46	3	-25	40.5	3155	34
440	G 19		11	49	20	-31	12.0	16055	35
440	G 25	MCG-5-28-14	11	50	36	-32	17.3	8193	28
440	G 26		11	50	48	-32	22.3	8187	32
440	G 32		11	54	9	-32	6.4	8091	34
504	G 30		11	54	42	-27	25.3	1772	37
440	G 37	MCG-5-28-18	11	56	44	-28	37.6	2080	32
440	G 38	MCG-5-29-1	11	59	9	-31	25.5	2373	24
442	G 3	MCG-5-30-4	12	30	46	-31	5.1	15572	26
442	G 6		12	31	27	-30	56.4	5836	26
322	G 30	N 4553	12	33	26	-39	9.8	3160	23
381	G 5		12	37	51	-36	41.7	5698	30
381	G 17		12	41	52	-33	38.0	3110	38
507	G 14	MCG-4-30-21	12	45	40	-26	11.5	3361	25
323	G 41	N 4767 B	12	51	58	-39	34.9	3499	29
507	G 55	N 4831	12	54	55	-27	1.3	3320	27
443	G 17	MCG-5-31-7	12	55	2	-29	29.8	3085	25
381	G 35		12	56	13	-32	41.4	10593	35
443	G 29	MCG-5-31-14	12	58	36	-32	7.9	9414	26
381	G 50	MCG-5-31-199	12	59	22	-32	31.1	9346	29
507	G 69		13	0	3	-26	23.8	13817	37
443	G 42	MCG-5-31-25	13	0	46	-29	33.5	2906	39
382	G 3	MCG-5-31-27	13	0	48	-32	35.9	4831	30
443	G 53	MCG-5-31-29	13	1	47	-29	54.0	3837	34
443	G 54	MCG-5-31-30	13	2	6	-29	58.5	3188	25
508	G 1		13	2	11	-25	6.6	6212	32
382	G 6		13	2	47	-32	41.5	4809	36
443	G 59	MCG-5-31-32	13	2	52	-28	11.5	3473	34
443	G 75	N 4980	13	6	26	-28	22.4	1456	31
443	G 79		13	7	38	-27	42.3	2135	40
443	G 80	MCG-5-31-38	13	8	25	-27	44.6	2164	37

TABLE I. (continued)

ESO	NO.	OTHER ID.	R.A. H	M	S	DEC. °	'	V (KM/S)	±
508	G 25		13	8	25	-25	38.0	13556	50
443	G 85		13	12	27	-31	59.3	2399	39
444	G 2		13	14	0	-27	37.4	1648	35
508	G 34	MCG-4-31-45	13	14	13	-25	4.4	1938	37
508	G 44	MCG-4-31-51	13	16	43	-26	44.1	9891	27
508	G 51	MCG-4-32-6	13	17	45	-25	49.4	2153	25
508	G 54		13	18	2	-27	21.3	8209	37
444	G 12	MCG-5-32-1	13	18	4	-29	13.1	4268	25
444	G 14		13	19	21	-30	26.9	5674	65
444	G 15	MCG-5-32-3	13	19	36	-30	48.8	4512	38
508	G 60	I 4231	13	20	28	-26	2.4	2291	30
444	G 21		13	20	43	-29	51.2	4317	40
444	G 22		13	20	58	-27	43.8	13777	31
324	G 16		13	21	17	-39	.1	14804	33
444	G 25	MCG-5-32-7	13	21	18	-31	24.5	14459	27
382	G 58	MCG-5-32-11	13	22	23	-33	23.8	7759	27
508	G 72	MCG-4-32-11	13	22	29	-25	5.6	10416	23
444	G 33	MCG-5-32-15	13	23	16	-31	52.2	2454	31
509	G 5	MCG-4-32-15	13	23	49	-26	28.9	9896	33
444	G 34	I 4247	13	23	57	-30	6.2	274	65
509	G 12		13	24	19	-26	44.0	14357	30
444	G 42	I 4253	13	24	46	-27	36.7	10197	27
509	G 19	MCG-4-32-19	13	25	11	-25	35.8	10759	27
509	G 24		13	25	34	-25	33.9	13043	33
444	G 47	MCG-5-32-28	13	25	36	-31	36.0	4453	31
509	G 26		13	25	38	-27	18.7	12949	31
383	G 2		13	25	45	-37	18.9	6171	35
444	G 51	I 4259	13	26	40	-29	52.6	14196	29
444	G 57	I 4264	13	27	31	-27	40.2	3513	31
444	G 58	I 4262	13	27	36	-28	.8	10494	30
509	G 35	I 4267	13	27	50	-25	59.9	4494	32
444	G 65	I 4273	13	28	42	-28	38.2	12956	29
444	G 66		13	29	2	-31	39.8	4505	44
509	G 49	I 4281	13	29	49	-26	54.7	11968	42
509	G 61	I 4288	13	31	43	-27	2.9	10480	28
444	G 74	I 4290	13	32	32	-27	46.0	4869	26
444	G 77		13	33	3	-30	10.6	3847	53
383	G 37	MCG-5-32-48	13	33	14	-32	45.4	3563	32
509	G 80	I 4298	13	33	48	-26	17.9	6732	31
444	G 86	MCG-5-32-56	13	35	7	-30	40.8	4168	29
324	G 44		13	35	10	-39	35.3	2544	30
444	G 87	MCG-5-32-57	13	35	22	-31	9.8	4356	26
445	G 5	MCG-5-32-61	13	37	7	-32	20.5	4028	33
509	G 91	I 4315	13	37	16	-25	13.3	5152	35
445	G 14	MCG-5-32-67	13	39	18	-30	30.8	4749	29
445	G 15	MCG-5-32-68	13	39	24	-30	47.2	4417	26
445	G 17	I 4318	13	40	33	-28	43.0	8946	29
509	G 98		13	40	34	-25	40.8	8001	27
445	G 19	I 4319	13	40	36	-29	33.2	4686	31
509	G1 0	MCG-4-32-52	13	41	3	-27	6.6	6567	32
509	G1 1	I 4320	13	41	15	-26	58.8	6827	37
445	G 27	MCG-5-33-3=I 4	13	44	25	-28	4.9	11493	27
445	G 35	MCG-5-33-10	13	45	20	-30	12.2	4912	41
445	G 39	N 5298	13	45	45	-30	10.8	4420	29

TABLE I. (continued)

ESO NO.		OTHER ID.	R.A.			DEC.		V	+ -
			H	M	S	O	'	(KM/S)	
445	G 41	I 4327	13	45	53	-29	58.1	5413	36
383	G 88		13	46	40	-32	49.3	4262	37
445	G 57	MCG-5-33-24	13	48	17	-30	32.0	5641	33
445	G 58	MCG-5-33-25	13	48	27	-30	54.1	5070	27
510	G 4		13	48	43	-26	23.1	7361	39
445	G 66		13	49	58	-30	27.9	7269	32
445	G 69		13	50	17	-30	28.0	6892	27
445	G 73		13	51	7	-29	36.8	6853	27
510	G 7	MCG-4-33-7	13	51	8	-27	22.6	5583	33
384	G 10		13	51	14	-32	39.4	4415	37
510	G 11	MCG-4-33-10	13	51	37	-26	19.8	5892	28
445	G 76		13	52	4	-28	53.5	2717	36
445	G 80	MCG-4-33-16	13	53	23	-27	30.2	15123	32
445	G 81	MCG-5-33-33	13	53	41	-32	23.3	4348	32
445	G 87	N 5393	13	57	41	-28	38.0	6019	26
510	G 40	MCG-4-33-28	13	58	31	-25	57.4	6364	39
510	G 42	MCG-4-33-30	13	58	43	-25	.6	6260	39
510	G 46	MCG-4-33-32	13	59	9	-25	17.9	6389	26
446	G 1	MCG-5-33-40	14	0	22	-31	6.5	7144	24
446	G 3		14	0	56	-31	42.6	7104	24
510	G 54	MCG-4-33-36	14	1	13	-25	58.5	6094	25
325	G 51	I 4367	14	2	35	-38	58.0	4110	27
384	G 53		14	3	38	-34	4.5	4881	22
510	G 69	I 4374	14	4	39	-26	46.8	6534	25
446	G 17	MCG-5-33-47	14	5	4	-31	48.8	4168	25
511	G 21	MCG-4-34-4	14	15	21	-27	11.1	7746	26
511	G 23	MCG-4-34-5	14	15	34	-27	8.9	6796	28
511	G 31		14	16	30	-27	8.4	6689	32
511	G 32	MCG-4-34-11	14	16	37	-27	8.7	6421	33
511	G 34	MCG-4-34-13	14	18	20	-27	2.0	6508	28
580	G 16	N 5734	14	42	19	-20	39.6	4098	26
580	G 39	N 5761	14	46	18	-20	10.2	4106	26

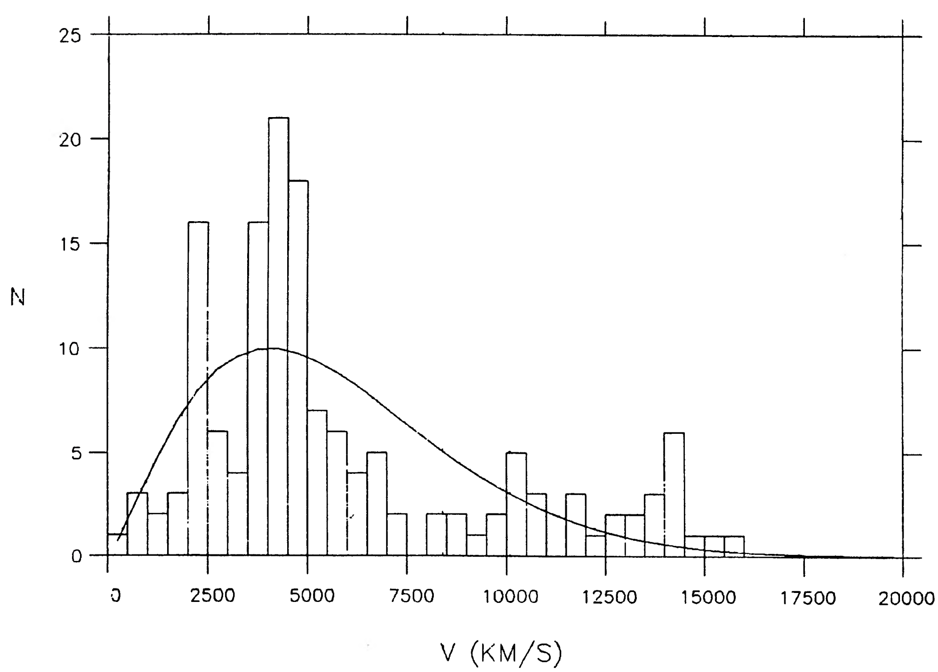

FIG. 1. Histogram of redshifts in 500 km s^{-1} intervals in the region $13^h \leqslant \alpha \leqslant 14^h$ and $-25° \leqslant \delta \leqslant -33°$ of the survey (region I). The solid curve denotes the expected distribution for a uniform magnitude-limited sample.

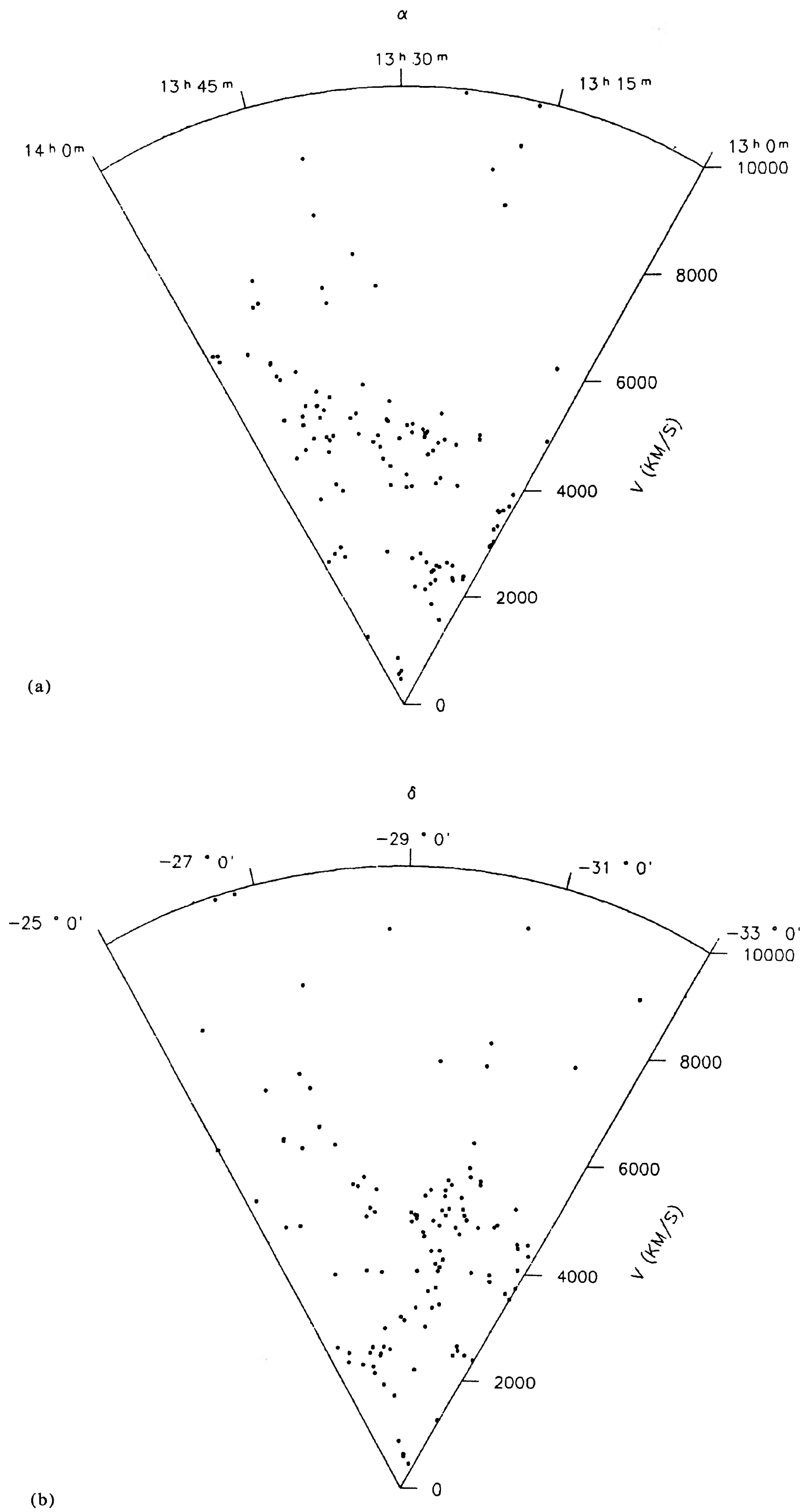

FIG. 2. Map of velocity versus right ascension (a) and declination (b). The objects plotted are in region I and have $m_B \leqslant 15.0$ and $v \leqslant 10\,000$ km s^{-1}.

culated for the present sample. The space density derived utilizing the $m_B \leqslant 15.0$ sample is shown in Fig. 3 for $r > 10h^{-1}$ Mpc to avoid a large peak associated with a nearby group at 500 km s^{-1}. Besides the large fluctuation associated with another group at 2000 km s^{-1}, there is an overdensity produced by the clustering of galaxies at about 4000 km s^{-1} which extends from approximately 30 to $60h^{-1}$ Mpc with a peak density of roughly six times the mean spatial density in the surveyed volume. The unbiased estimate of $n(r)$ also confirms our earlier claim for the existence of a region of below-average galactic density, which extends over at least $30h^{-1}$ Mpc. The mean number density within the volume defined by the solid angle of region I and $r \leqslant 100h^{-1}$ Mpc was calculated using the unbiased estimator introduced by DH

$$n_1 = \frac{\int [N(r)/\phi(r)]dr}{\int dV} = 15 \times 10^{-3} \text{ gal Mpc}^{-3}. \qquad (2)$$

This value of n_1, plotted in Fig. 3, is comparable to that estimated by DH for a much larger volume.

In order to search for a dispersed population connecting the Centaurus and Hydra complexes, we have also surveyed a region $15° \times 6°$, centered at $\alpha = 11^h\ 30^m$ and $\delta = -30°$. The radial-velocity distribution for the galaxies with $m_B \leqslant 15.0$ in this region is compared to the expected distribution of a uniform sample in Fig. 4. The histogram shows two peaks, one at about 1750 km s^{-1} (15 members), associated with the NGC 3923 group originally identified by de Vaucouleurs (1975), and a background structure at $\sim$8500 km s^{-1}. However, in the velocity range 3000 to 7000 km s^{-1}, there are only three galaxies, whereas about 16 would be expected for a spatially homogeneous distribution. Figure 5 shows plots of velocity versus right ascension and declination for the galaxies brighter than $m_B = 15.0$ in region II. The small number of objects in the velocity range typical of the galaxies in Hydra and Centaurus is in agreement with the result of the percolation analysis (Paper I) which showed no evidence of a dispersed population connecting the complexes of Hydra and Centaurus. If there is any connection between the two systems, it is probably in the form of a localized and very low-density structure, such as the bridge claimed to exist by Hopp and Materne (1985) farther south in the declination zone between $-30°$ and $-40°$. Within the observed solid angle, apart from the nearby group, we find a large region apparently devoid of galaxies. However, the significance of this low-density region must await further observations over an enlarged area of the sky. Furthermore, the concentration of galaxies around 8500 km s^{-1} is rather dispersed, showing no indication of prominent clustering.

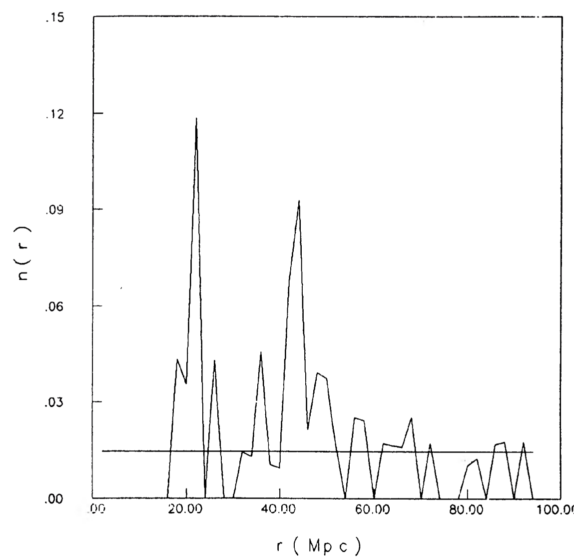

FIG. 3. Radial variation of the spatial density of bright ($M_B \leqslant -18.5$) galaxies within the solid angle of region I. Also plotted is the estimate n_1 for the mean galactic density in the surveyed volume.

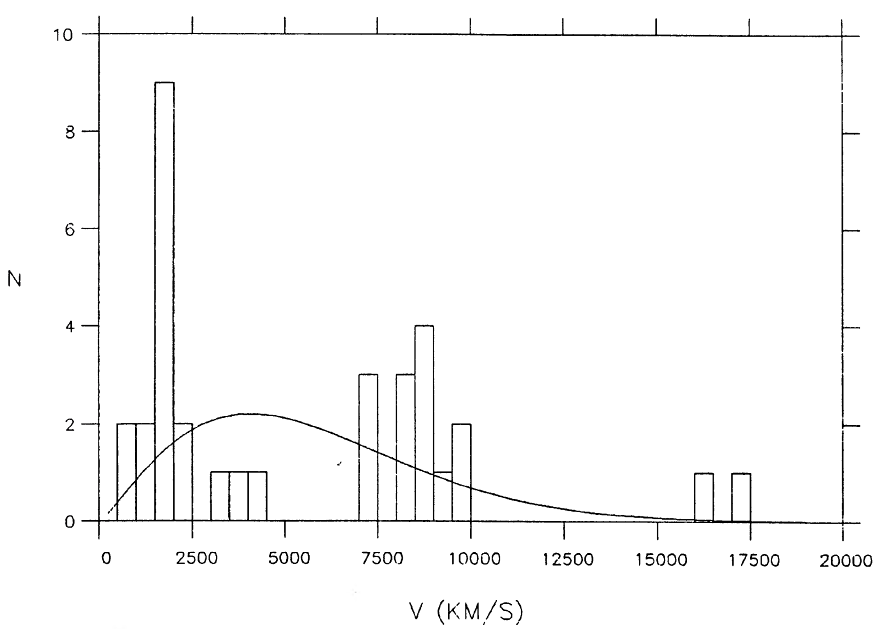

FIG. 4. Histogram of redshifts in 500 km s^{-1} intervals for region $11^h \leqslant \alpha \leqslant 12^h$ and $-33° \leqslant \delta \leqslant -27°$ (region II), compared to the expected distribution of a uniform sample represented by the solid line.

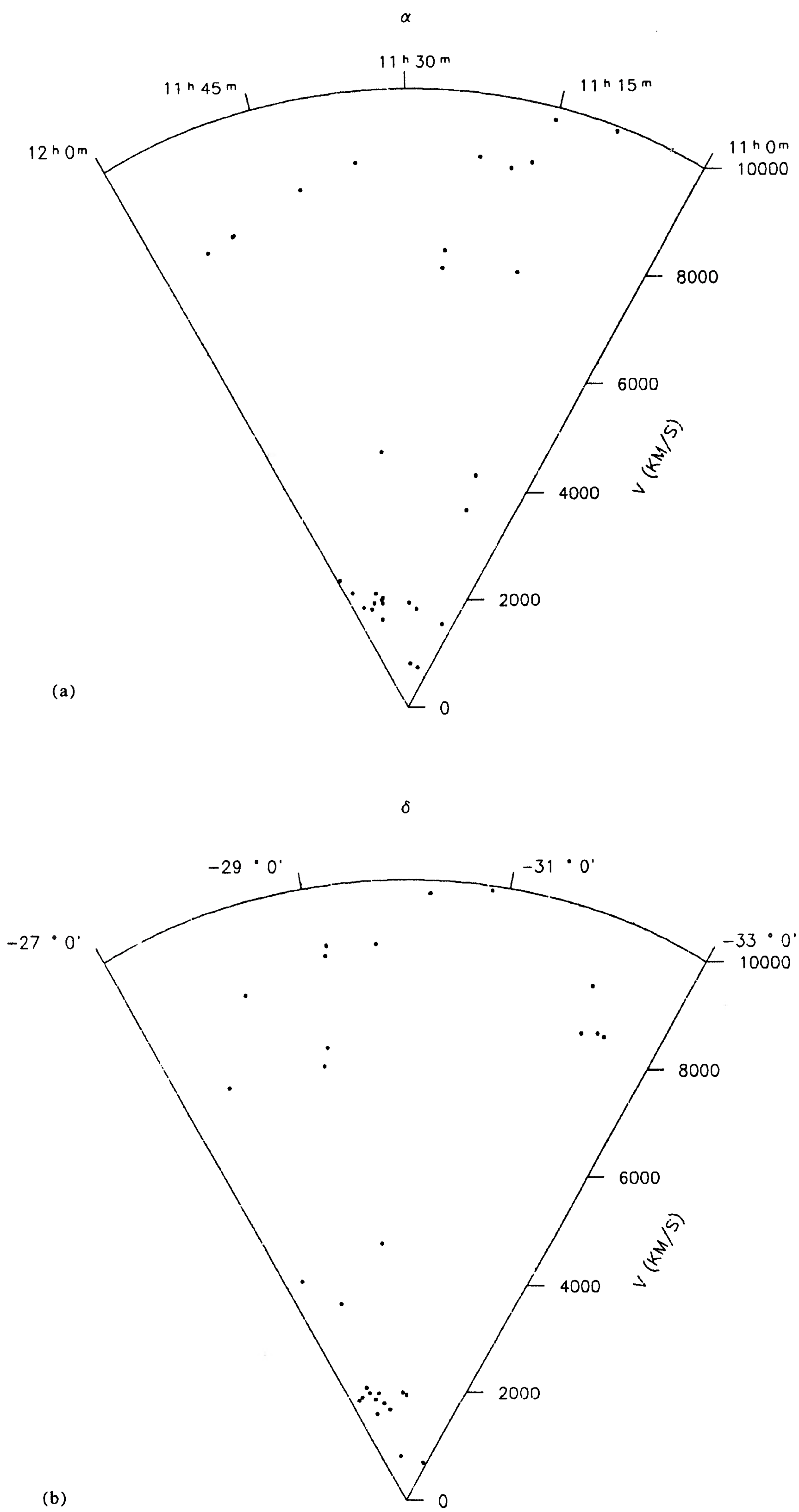

FIG. 5. Map of velocity versus right ascension (a) and declination (b) for galaxies in region II. The 31 galaxies plotted have $m_B \leqslant 15.0$ and $v \leqslant 10\,000$ km s^{-1}.

b) Distribution of Galaxies in the Centaurus Complex

In order to investigate the relationship between the structure observed in region I with the Centaurus cluster, it is necessary to examine the distribution of galaxies over a larger area of sky. For this purpose, we show in Fig. 6 the projected distribution of galaxies in the region defined by $12^h15^m \leqslant \alpha \leqslant 14^h15^m$ and $-44° \leqslant \delta \leqslant -21°$, which includes the Centaurus cluster proper and region I. We have used different symbols to indicate galaxies with and without redshifts, and only show galaxies with $m_B \leqslant 14.5$. This sample with a brighter magnitude limit is used because it is better suited for a preliminary investigation of the overall system, since it is significantly more complete for this larger area. The sky distribution of galaxies with measured radial velocities is given for four consecutive redshift intervals in Fig. 7. The nearest window is dominated by the foreground NGC 5128 group at about 500 km s^{-1}. The main part of the Centaurus cluster appears in the window $2000 < v \leqslant 4000$ km s^{-1}. In this velocity range there are also some other small groups from 13^h to 14^h and from $-22°$ to $-34°$, apparently forming, with Centaurus, a larger structure extending over at least $12h^{-1}$ Mpc towards the northeast. The concentration of galaxies in this region stretches $\sim 20h^{-1}$ Mpc in depth, and forms the main concentration of galaxies in the interval $4000 < v \leqslant 6000$ km s^{-1}. In this figure we still see galaxies of the Centaurus cluster which probably belong to the second component of the Cen 30-Cen 45 binary system, as suggested by Lucey *et al.* (1986). Finally, in the last window ($6000 < v \leqslant 10\,000$ km s^{-1}), there are relatively few galaxies over the entire region, suggesting that the empty region detected in the direction of region I may extend over a larger area of the sky, but this must be confirmed by future observations.

Although the sample is not complete, and the sky coverage is not uniform, the observed distribution in the different redshift windows strongly suggests that the structure detected in region I is probably part of a much larger system, situated within $60h^{-1}$ Mpc, which also contains the Centaurus cluster. This supercluster may extend to the north, to join with the filament No. 13 detected by Moody *et al.* (1983), as proposed by Chincarini (1984), and towards the south, across the galactic plane to the Telescopium-Pavo-Indus complex, as suggested by Fairall (1984). Preliminary results of group analysis of the galaxy distribution indicate that it is apparently formed by chains of groups and "isolated" galaxies, similar to the structure of superclusters described in earlier works (e.g., Oort 1983).

IV. DISCUSSION

In this paper, we have investigated the spatial distribution of galaxies in the vicinity of the Centaurus cluster, as part of an ongoing effort to study the structural properties of the Centaurus-Hydra supercluster. The present work, which in a sense complements that of Hopp and Materne (1985) in

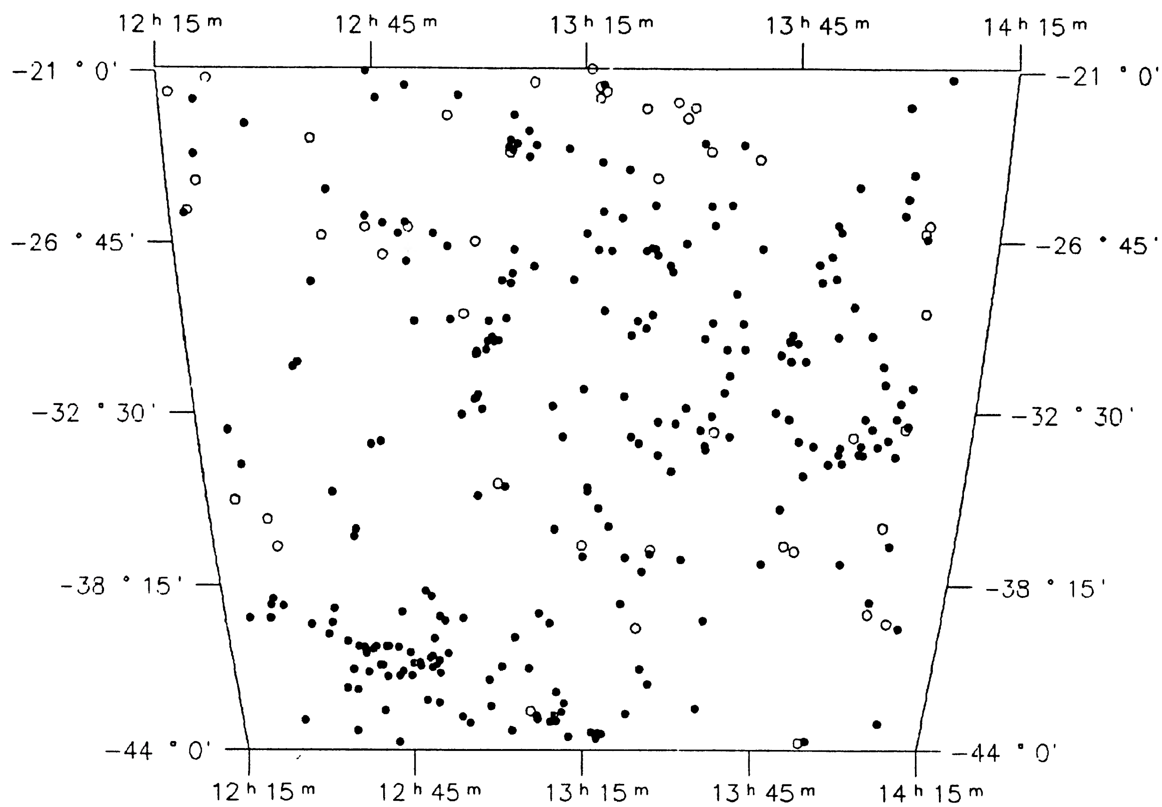

FIG. 6. Projected distribution of the 304 galaxies with $m_B \leqslant 14.5$ in the region bounded by $12^h15^m \leqslant \alpha \leqslant 14^h15^m$ and $-44° \leqslant \delta \leqslant -21°$. The symbols denote galaxies with (●) and without (○) measured radial velocities.

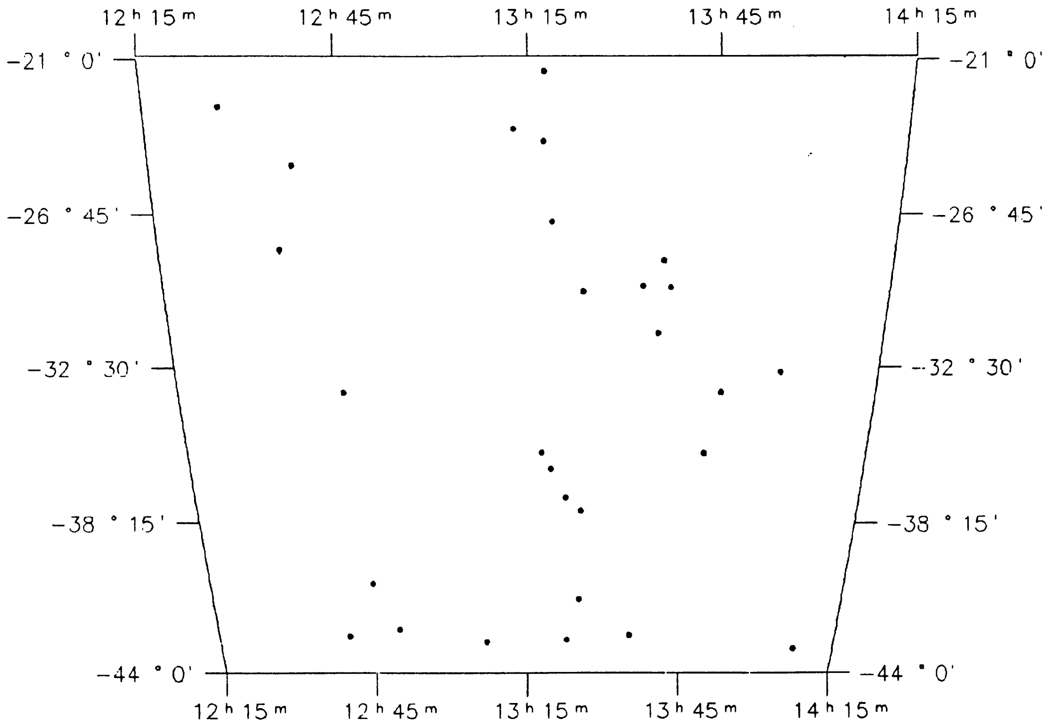

(a)

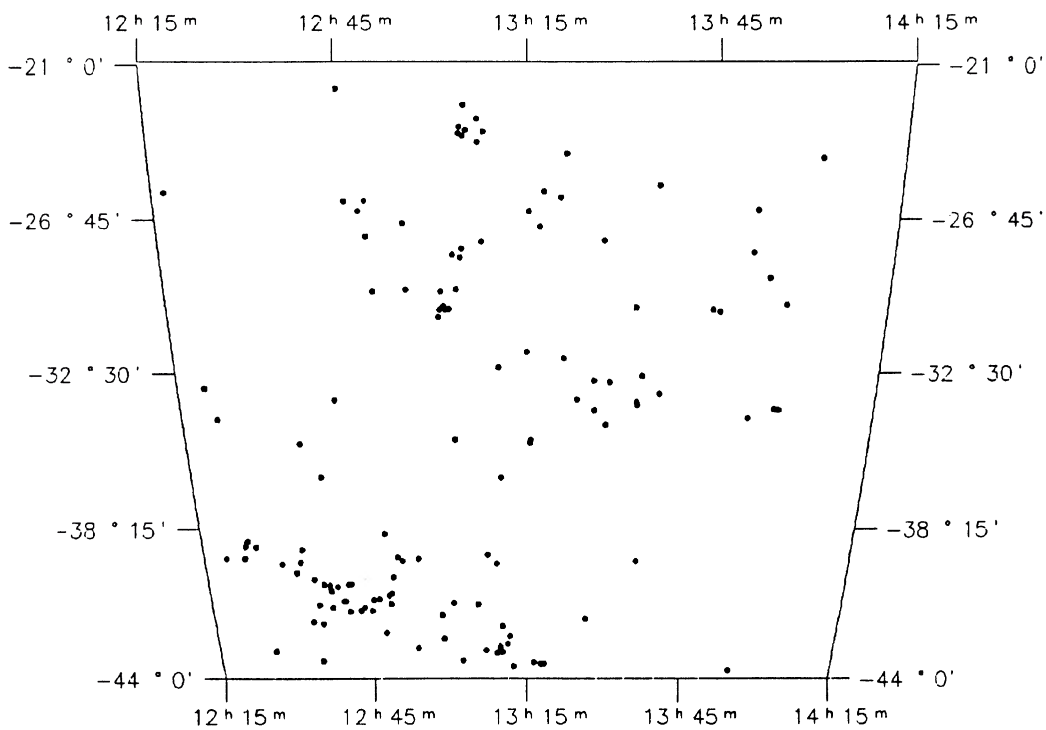

(b)

FIG. 7. Distribution of galaxies with redshifts in the region of Fig. 6 in four consecutive redshift windows in intervals of 2000 km s^{-1}, except the last one (d), which includes galaxies in the range $6000 < v \leqslant 10\,000$ km s^{-1}.

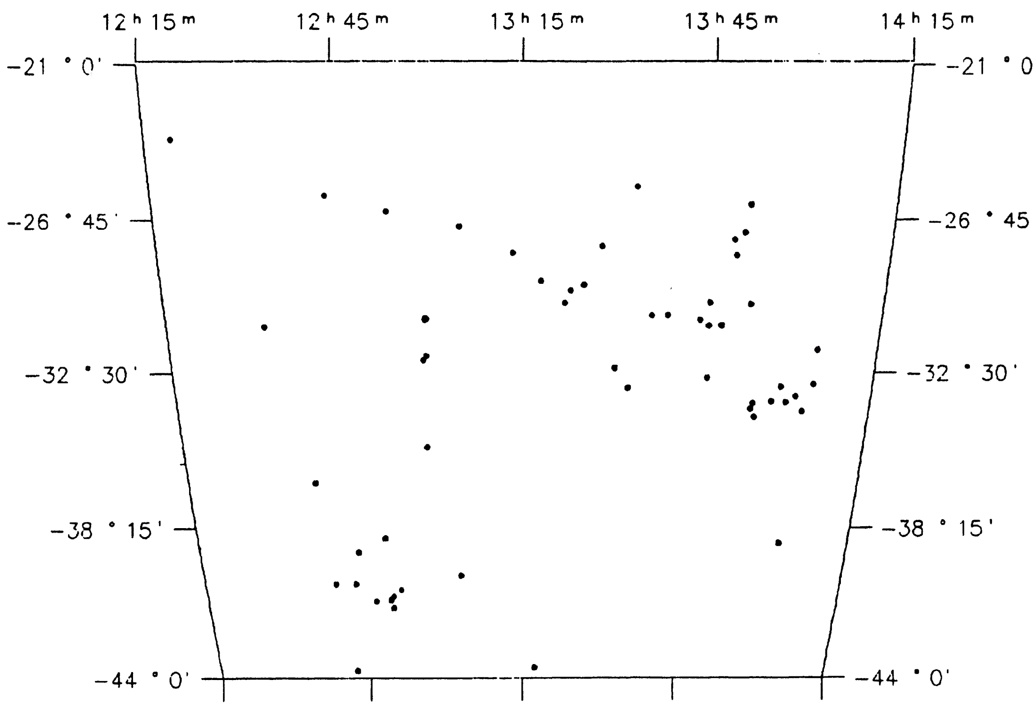

(c)

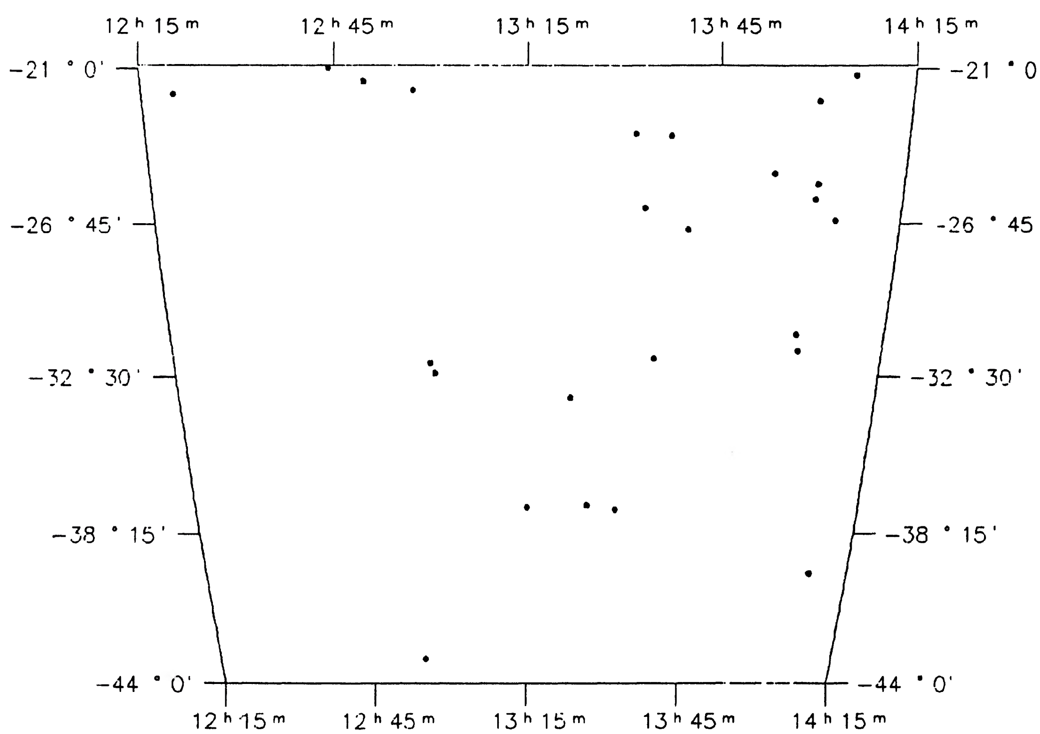

(d)

FIG. 7. (continued)

the Antlia region, used nearly complete redshift data for galaxies in two distinct areas of the sky to probe the large-scale environment of the Centaurus cluster.

In region I, located to the northeast of the Centaurus cluster, we have found evidence of a significant concentration of galaxies that may be an extension of a supercluster associated with the Centaurus system. The distribution of galaxies in this region stretches some $30h^{-1}$ Mpc in depth and surrounds a void which, with the present sky coverage, is still poorly surveyed. This distribution seems to be connected to the Centaurus cluster proper at about $v = 3500$ km s^{-1} by a sparse population, essentially confirming the results of the two-dimensional analysis presented in Paper I. This supercluster is formed by several aggregates of galaxies, the most important being Centaurus, Klemola 27, and the NGC 5419 group.

From the data gathered in region II, we find no evidence of a low-density dispersed population connecting the structure associated to Centaurus with the Hydra complex. This result suggests that the complexes of Centaurus and Hydra are neither imbedded in a low-density dispersed component, nor do they surround a sheet of field galaxies. If a connection between both complexes exists, it is probably in the form of a localized low-density bridge such as that between the regions of Antlia and Centaurus, claimed to exist by Hopp and Materne (1985). Therefore, it may be more appropriate to consider the complexes of Hydra and Centaurus as two distinct superclusters.

In both regions studied we have detected the presence of low-density regions of some significance, especially the one situated behind the Centaurus supercluster, spanning at least 3000 km s^{-1}, and the one located between it and the Hydra complex, about 5000 km s^{-1} deep. The density contrast in these regions is estimated to be in the range 0.2–0.3, comparable with that of 0.25 for the void in Bootes. However, since the present surveys cover small areas of the sky, it is difficult from the present data to map these voids in detail and to establish more precisely their characteristics.

Clearly, a more thorough investigation of the extension, geometry, and morphology of the Centaurus supercluster and the Centaurus-Hydra complex as a whole requires more observations. Meanwhile, smaller surveys would be useful to investigate the possible extensions of the Centaurus complex to the north, joining with the area covered by the CfA Redshift Survey, and to the south, towards the Telescopium-Pavo-Indus system of galaxies at approximately the same redshift as the Centaurus cluster.

We would like to thank all the people involved in the redshift survey effort, in particular, M. A. Nunes, M. Maia, R. Carvalho, and C. Rité. We would also like to thank D. Latham and J. Geary for their continuing support to our redshift survey, and to J. Menzies and A. Fairall for communicating in advance of publication their observations in the regions of interest. We would also like to thank J. Cowan for his contribution in the early part of this project and his comments on the present manuscript.

REFERENCES

Chincarini, G. (1984). In *Clustering and Substructures*, IAU Colloquium No. 78, edited by M. Capaccioli (Reidel, Dordrecht).
Chincarini, G., and Rood, H. J. (1979). Astrophys. J. **230**, 648.
da Costa, L. N., Nunes, M. A., Pellegrini, P. S., Willmer, C., Chincarini, G., and Cowan, J. (1986). Astron. J. **91**, 6 (Paper I).
da Costa, L. N., Pellegrini, P. S., Nunes, M. A., Willmer, C., and Latham, D. W. (1984) Astron. J. **89**, 1310.
Dickens, R. J., Currie, M. J., and Lucey, J. R. (1986). Mon. Not. R. Astron. Soc. **220**, 679.
Fairall, A. P. (1984). Publ. Dept. Astron. Univ. Cape Town No. 6.
Fouqué, P., and Paturel, G. (1985). Astron. Astrophys. **150**, 192.
Geller, M. J., and Huchra, J. P. (1983). Astrophys. J. Suppl. **52**, 61.
Hopp, U., and Materne, J. (1985). Astron. Astrophys. Suppl. **61**, 93 (HM).
Huchra, J. P. (1976). Astron. J. **81**, 952.
Huchra, J. P., Davis, M., Latham, D., and Tonry, J. (1983). Astrophys. J. Suppl. **52**, 39.
Lauberts, A. (1982). *The ESO / Uppsala Survey of the ESO(B) Atlas* (European Southern Observatory, Munich).
Lucey, J. R., Currie, M. J., and Dickens, R. J. (1986). Mon. Not. R. Astron. Soc. **221**, 453.
Moody, J. E., Turner, E. L., and Gott, J. R. (1983). Astrophys. J. **273**, 16.
Oort, J. H. (1983). Annu. Rev. Astron. Astrophys. **21**, 373.
Richter, O. G. (1984). Astron. Astrophys. Suppl. **58**, 131.
Richter, O. G., and Huchtmeier, W. K. (1983). Astron. Astrophys. **125**, 187.
Richter, O. G., Materne, J., and Huchtmeier, W. K. (1982). Astron. Astrophys. **111**, 193.
Sadler, E. M. (1984). Astron. J. **89**, 23.
Schechter, P. (1976). Astrophys. J. **203**, 297.
Tammann, G. A., and Sandage, A. (1985). Astrophys. J. **294**, 81.
de Vaucouleurs, G. (1975). In *Galaxies and the Universe*, edited by A. Sandage, M. Sandage, and J. Kristian (University of Chicago, Chicago).
de Vaucouleurs, G., and de Vaucouleurs, A. (1964). *Reference Catalog of Bright Galaxies* (University of Texas, Austin).
de Vaucouleurs, G., de Vaucouleurs, A., and Corwin, H. (1976). *Second Reference Catalog of Bright Galaxies* (University of Texas, Austin).